Available online at www.sciencedirect.com

ScienceDirect

Ciência & Tecnologia dos Materiais 27 (2015) 100–107

Ciência & Tecnologia dos MATERIAIS

http://ees.elsevier.com/ctmat

Special Issue IJSI 2014

Influence of the geometry on the fatigue performance of crenellated fuselage panels

Jin Lu*, Norbert Huber, Nikolai Kashaev

Institute of Materials Research, Materials Mechanics, Helmholtz-Zentrum Geesthacht, Max-Planck-Str. 1, 21502 Geesthacht, Germany

Abstract

Crenellation is a novel local engineering technique aimed at improving the fatigue performance of the airframe structures without increasing the weight. In this concept, a systematic thickness variation is applied to the fuselage skin to retard the fatigue crack growth. In order to achieve the best retardation effect, it is necessary optimize the crenellation geometry. As a result, a parameter study characterizing three independent geometric aspects of the crenellations was performed: the crenellation ratio c, the periodic length λ and a position parameter. The study was based on a FEA model validated by experiments. It is expected to give a sufficiently accurate prediction on fatigue life of different crenellation patterns. The obtained knowledge concerning the impact of those geometrical factors could provide guidance for future crenellation designs for industrial applications.

Keywords: fatigue life improvement; airframe structure; crenellations; geometric optimization

1. Introduction

Crenellation is an innovative concept aimed at improving the fatigue performance of fuselage panels with laser-beam welded stringers (Fig. 1) [1-6]. In this concept, the thickness of the fuselage skin is systematically varied while the structural weight remains unchanged. The purposely increased and reduced skin thickness introduces peaks and valleys in the stress intensity factor (SIF) profile along the crack path (Fig. 1c), which accordingly accelerate and retard the fatigue crack propagation as dictated by the Paris Law:

$$\frac{da}{dN} = C\Delta K^m \qquad (1)$$

where da/dN is the fatigue propagation rate and ΔK is the SIF range during a load cycle. In a well-designed crenellation, the fatigue life gain in the retardation region is much larger than the fatigue life loss in the acceleration region. This leads to an overall fatigue life improvement. Uz et al. [1,2] experimentally investigated the fatigue life improvement in crenellated fuselage panels with and without welded stringers (the crenellation geometry applied is depicted in Fig.1). In their experiments fatigue cracks were assumed to initiate at the welding site of the middle stinger in the center of the panel. It was demonstrated that from an initial half crack length of 37.5 mm to a final half crack length of 225 mm, the application of crenellations lead to a 9% increase of fatigue life in the un-stiffened panels and a 65% increase in stringer-stiffened panels.

The fatigue life improvement brought by crenellations is governed by the shape of the modified SIF profiles, which is in turn determined by the geometries of the crenellations. Thus it is necessary to identify the optimum geometric design of crenellations with the best fatigue resistance for future industrial applications. This aim can be achieved with the help of the finite element analysis (FEA), which is the well-established technique for estimating the SIF of cracks

* Corresponding author.

E-mail address: jin.lu@hzg.de (J. Lu)

http://dx.doi.org/10.1016/j.ctmat.2015.06.003

in complex structures. Successful assessments of the fatigue performance of structures based on FEM simulation can be found in the work of previous researchers such as the assessment of integrally stiffened structure by Häusler et al. [7]. Once the reliability of the FEA models of a crenellated structure is validated by experiment in fatigue life prediction, it can be used to evaluate the fatigue performance of different crenellation patterns with arbitrary geometric designs.

The previous study on the geometric optimization for crenellated structures is rather limited. Uz *et al*. [8] did some optimization work by an approach coupling FEA with artificial neutral network methodologies. It was found the fatigue life is always improved by the introduction of crenellations. In addition the improvement of fatigue life is enhanced by increasing the thickness ratio between the thick and thin regions at a constant area ratio between the two regions.

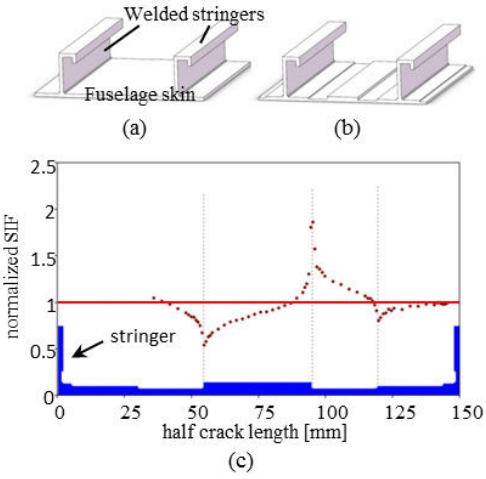

Fig. 1. (a) Flat and (b) crenellated structure with the same weight. (c) SIF profile of a center through crack in crenellated stiffened panel normalized to the SIF values of a reference panel (red line) with the same structural weight (after [1]).

However, the optimization of Uz et al. was limited to one specific configuration (one pad-up between each two stringer as depicted in Fig. 1b) [8], in which the parameters optimized are from the detailed geometrical dimensions in this configuration. In this study feature-based parameters are used, each of which independently describe one characteristic aspect of crenellations. Those parameters can define the crenellation pattern with more flexibility and thus allow a broader exploration of the solution space.

2. Experimental

2.1. Approaches of this study

The aim of the study in extension to previous work is to investigate the fatigue performance of crenellated panels under biaxial loads, which is the typical loading state of the fuselage skin under service conditions. The long-term cyclic loading due to the repetitive fuselage pressurizations, which is closely related with the fatigue problem of the fuselage [9, 10], can be experimentally realized by using the biaxial testing machine and cruciform specimens. FEA models for such an experimental setup were established and validated by biaxial fatigue tests carried out on flat and crenellated panels. After validation, new crenellation patterns with varied geometric parameters were implemented in the models, from which the SIF profiles with crack extension were extracted. Based on the SIF profiles fatigue life of corresponding crenellated structures were estimated by integrating the inverse of da/dN expression according to equation 1, that is :

$$N = \int_{a_0}^{a_f} \frac{1}{C\Delta K^m} da \qquad (2)$$

where N is the number of cycles to grow the crack from initial length of a_0 to a final length of a_f. The influence of those geometric parameters on fatigue life can be thus identified.

2.2. Specimens and experimental setup

In this work biaxial fatigue tests were firstly carried out on two flat panels (thickness: 1.9 mm, 2.9 mm) and a crenellated panel (equivalent thickness: 2.9 mm) in order to validate the FEA models (Table 1). Those validation tests were also part of the experimental work investigating the fatigue performance of crenellated structure under biaxial loading conditions, the results of which has been published in [11].

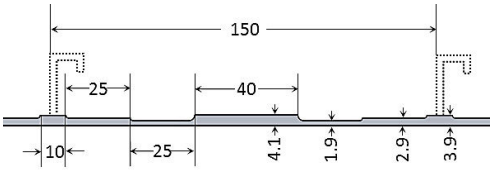

Fig. 2. Geometries of a crenellated sheet with welded stringers (unit: mm).

The specimens are 560 mm × 560 mm square panels, which were cut from a 4.5 mm thick AA2139 sheet with T351 heat treatment. The outer region of the

specimens retains the original thickness of the sheet. Four rows of 16 bolt holes were drilled along each rim of the specimens for fixation. In the center part of the specimens (400 mm × 400 mm square region) the panel was either milled symmetrically from both sides to 2.9mm in the reference panels or milled from one side to the corresponding dimension of crenellations in the crenellated panels. The milling process leads to a negligible value of compressive residual stress (<10 MPa) in the direction perpendicular to the crack plane. The detailed geometry of the investigated crenellation pattern is depicted in Fig. 2. In each bay between two stringers a centered thickened region with a thickness of 4.1mm was designed for crack retardation. The extra weight of this pad-up is compensated by two thickness reduction regions (1.9 mm) located on both sides. The sockets for the three stingers to be welded are marked by red lines in Fig.3b. In order to focus on the sole effect of the crenellations, in the present step of study stringers were not added in both the experiments and simulation.

In the center of the specimens, a pre-crack perpendicular to the major loading axis was introduced as shown in the inset of Fig. 3b. A hole with diameter of 1mm was firstly drilled at the panel center. Then a 12mm long and 0.6mm wide notch was made by electro discharge machining, which was symmetric to the center hole. Before subsequent fatigue tests strain gauges were applied on the specimens' surface. The positions of those strain gauges are indicated in the Appedix.

The specimens were tested with a biaxial servo-hydraulic testing machine (Fig. 3a), each load axis of which has a capacity of 1000 kN. The specimens were fixed in the horizontal plane by specially designed clamping devices (Fig. 3b), which can ensure a homogeneous stress distribution in the center part of specimens. Constant amplitude cyclic loading in both axes was applied to the specimens in phase with R ratio of 0.1. The maximum loads (Table 1) during a load cycle were adjusted according to the thickness of the panel to achieve a stress level similar to the real situation in fuselage skin during flight state. Since in a pressurized fuselage, the stress in the hoop direction of the fuselage is about twice of the stress in the axial direction, a biaxial load ratio of 0.5 is adopted in those fatigue tests. During the tests the positions of both crack tips were recorded at about every 1 mm of crack growth by a traveling camera underneath the specimens with an accuracy of 0.01mm. The fatigue crack propagation rate was obtained by the secondary polynomial fitting of 5 consecutive measurement points according to ASTM E647 [13].

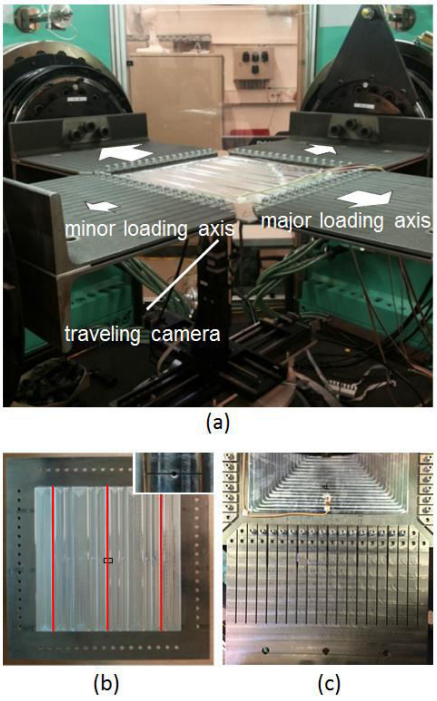

Fig. 3. (a) Experimental setup of the biaxial fatigue tests, (b) the specimen and (c) the specially designed clamping device.

Table 1. List of specimens.

specimens	Crenellation	thickness	maximum load-major	maximum load-minor
1	No	1.9 mm	55 kN	27.5 kN
2	No	2.9 mm	112.4 kN	56.2 kN
3	Yes	~2.9 mm	112.4 kN	56.2 kN

2.3. FEA modeling approach

A quarter FEA model for the experimental setup of the fatigue tests (Figure 3c) was established using the commercial code ABAQUS (version 6.12). Quadrilateral 4-node shell elements with reduced integration were applied to model the panels. The clamping device was modeled as a series of beams using quadratic 3-node beam elements. One end of each beam was tied to the position of corresponding bolt hole in the specimen panel with untied rotation freedoms. The other ends of the beams were kinetically coupled to a controlling point respectively, on which the maximum load in a load cycle was applied. As in the experiments, the clamping devices modeled were only allowed to move in the direction of loading axes with all other displacement and rotation

freedoms constrained. The mesh size near the final crack tips and along the crack path was refined to 1mm. The propagation of the crack was realized by sequential removing the symmetry boundary condition of the nodes at the crack tip along the crack line, which is situated at one symmetrical plane. The stress intensity factor (SIF) profile along crack path was obtained through the calculation of the strain energy releasing rate (SERR) using a two-step crack closure technique as described by Krueger [14]. In the simulation of the three fatigue tests as described in 2.2, the geometry of the specimen panel and the load were altered accordingly.

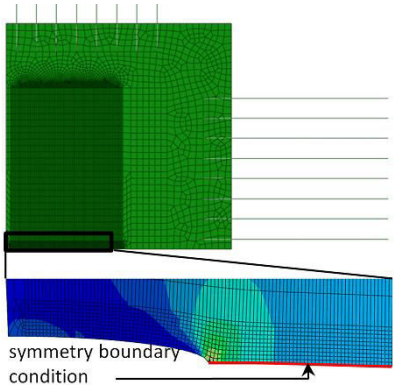

Fig. 4. Quarter FEM model of the experimental setup with 7476 nodes and 7341 elements.

3. Results and discussions

3.1. Validation of FEA model

The FEA model described in material and method part was validated by the 3 fatigue tests with different geometries (different panel thickness, with and without crenellation). The purpose is to confirm that those geometrical changes from specimen to specimen can be correctly reflected in the FEA model. To this end, the FEA models were firstly examined in terms of correctly characterizing the elastic deformation of the specimens, which is the precondition for an accurate estimation of the SIF. This was ensured by a good agreement (the deviations are mostly within 5%) between the strain measurements via the applied strain gauges in experiments and the strain values extracted from the corresponding locations in FEM models in simulations at the maximum load (Fig. 5).

Then the FEA model was further validated based on a cross-validation between different specimens. The experimentally measured fatigue crack propagation rates (da/dN) were plotted against the corresponding stress intensity factor ranges, ΔK, extracted from the simulations as shown in Figure 6a. The data points of all the three specimens fall into the same narrow scatter band with a linear trend as dictated by Paris Law. The Paris constants C and m were obtained through a linear fitting of the experimental data under double logrithm, which is marked by the black line in figure 6. Some deviations from this black line were observed in the crenellated specimen. They are either due to the occurance of stage III crack growth when ΔK is larger than 42MPa·m$^{1/2}$ (black circle) or due to the load history effects caused by the peaked ΔK profile at the two thickness steps of the crenellated specimen (red arrow) according to Uz *et al.* [1]. However, those deviations occur in rather localized regions, the overall fatigue life of all the three specimens can be predicted by the FEA model with good accuracy (the largest deviation is less than 10%) as shown in Figure 6b, c, d.

Based on the two validation steps the FEA model can be applied to study the SIFs and fatigue life of panels with different geometric details and, at the same time, to reduce the experimental cost to a minimum.

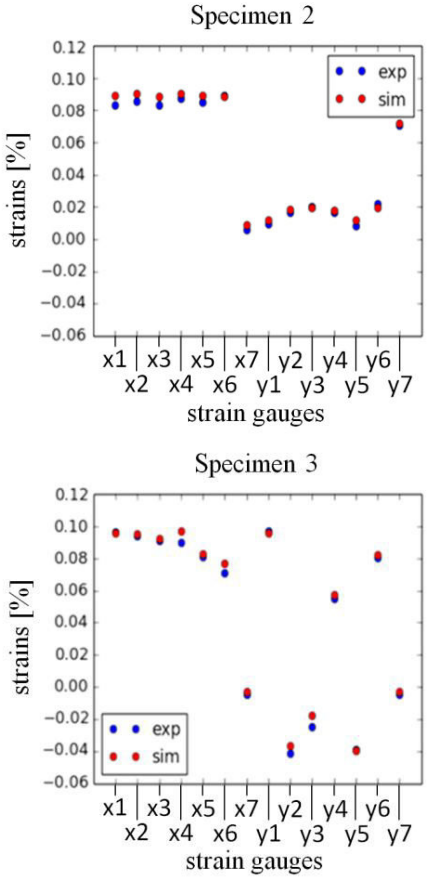

Fig. 5. Predicted and measured strains at different locations of tested specimens 2 and 3.

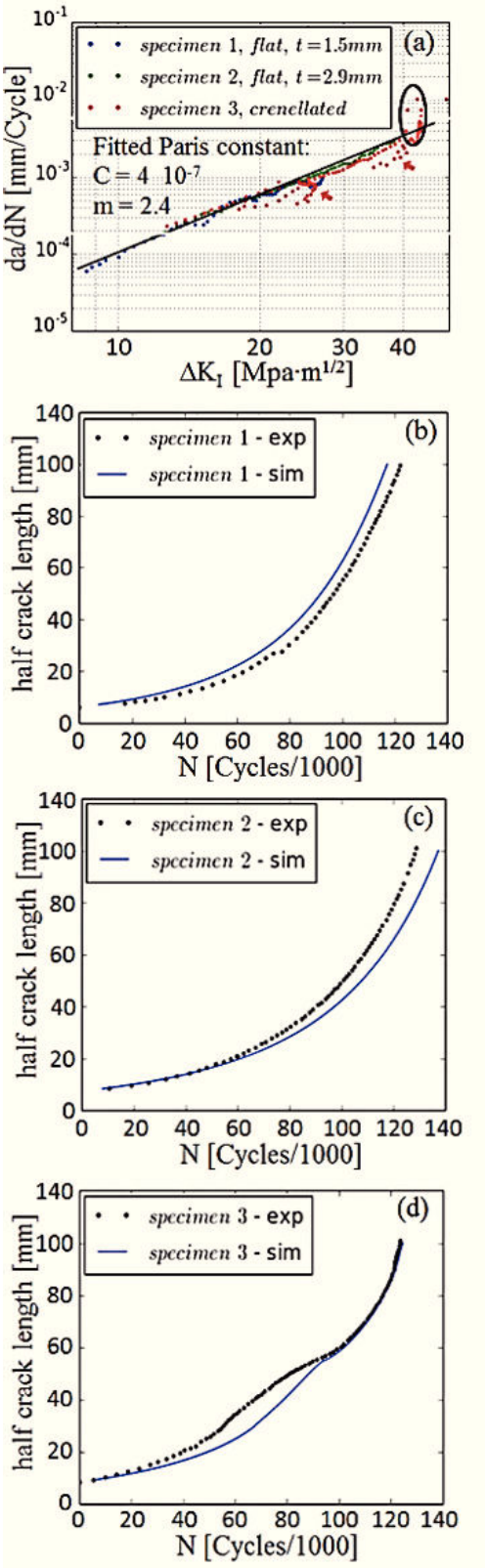

Fig. 6. (a) Paris Law and fitted Paris constants and (b-d) experimentally measured (exp) and predicted (sim) fatigue life.

3.2. Influence of geometric parameters of crenellations on the fatigue life improvement

A series of simulations were done using the calibrated model to evaluate the fatigue performance of crenellated panels with different crenellation patterns under the same biaxial loading condition as specimen 3. All of those crenellated panels are equivalent in weight to a flat reference panel with the thickness of 3 mm, the fatigue life of which is also calculated for comparison. In the middle of each panel a 12 mm initial crack was inserted inside a 16 mm x 400 mm rectangular region (green colored area in Fig. 7) where the thickness was kept the same as the reference panel. On both sides of this center region is the crenellated area (red colored area in Fig. 7), where the crenellation pattern is introduced as a periodic alternation of thick and thin regions symmetrically to the center line of the panel.

The geometry of the crenellation pattern can be fully defined by the widths of the thick and thin regions (w_1 and w_2) and the thickness of the two respective regions (t_1 and t_2) (Fig.8). In this work the parameters w_1 and w_2 are studied in a combined way, from which two new parameters are generated. The sum of w_1 and w_2 is defined as the periodic length λ. The ratio between w_1 and λ is defined as the crenellation ratio c, which ranges from 0 to 1 representing the cases from a flat panel to a crenellated panel with infinite high pad-ups (at the same time infinite small width of those pad-ups).

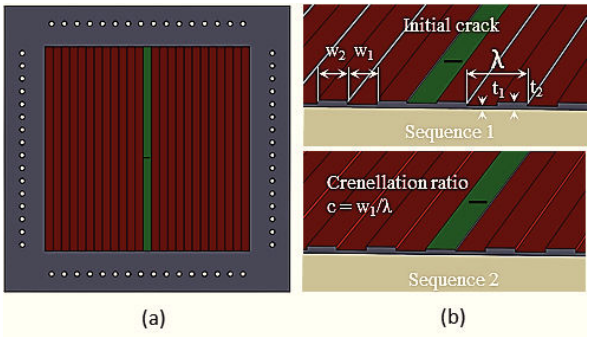

Fig. 7. (a) Geometry of the FEA model for the prediction of fatigue lives of different crenellation patterns (b) parameters used in this study to define the geometry of the crenellation pattern.

3.2.1 The influence of crenellation ratio c

In this part crenellation patterns with varying crenellation ratios from 0.25 to 0.75 were tested. All the investigated patterns have a periodic length of 32mm and the configuration of sequence 1 as shown in Figure 6b. Three representative results are displayed in Fig. 7 to show the general variation trend

of the predicted fatigue life and the corresponding SIF profiles with increasing crenellation ratios.

As shown in Fig.7, as c increases from 0.25 to 0.75 the predicted fatigue life remains almost the same although the corresponding SIF profiles are significantly different. The change in SIF profiles with increasing c is mainly in two aspects. On the one hand the valleys of SIF in front of a thick region become deeper, causing a stronger retardation of fatigue crack growth in this region. On the other hand, the peak in front of a thin region becomes higher and its root becomes broader due to the increased area of thin region, leading to a higher acceleration of fatigue crack growth. From the case of c=0.25 to the case of c=0.75, the increased retardation and acceleration of fatigue crack growth well counterbalance each other, which keeps the fatigue life nearly constant.

Although the crenellation ratio has no significant influence on the fatigue life within the tested c range, from manufacturing point of view the crenellated panels with lower crenellation ratio may be preferred. To achieve the same fatigue life improvement, only small grooves need to be made in panels with lower crenellation ratios while in the panels with high crenellation ratios, large area of the panel surface needs to be milled considering the large thinned area.

On the other hand, from the fracturing behaviour point of view, panels with large crenellation ratios seem more advantageous. As shown in Fig.7b, the higher the crenellation ratio is the deeper the valleys of SIF before the thick regions becomes. After the onset of fracturing, local SIF in those deep valleys could possibly fall below the fracture toughness of the material, which would stop the unstable propagation of a crack. Thus it is reasonable to assume that structures with higher crenellation ratio would have a better damage tolerance.

In the following investigations, the crenellation ratio of 0.5 was adopted representing the compromise between the two considerations.

3.2.2 The influence of relative positions of thick and thin regions

In this part the fatigue life of the previously discussed c = 0.5 case was recalculated with the configuration of sequence 2, which is a switch of positions between the thick and the thin regions with respect to the configuration 1. As shown in Fig. 9 the change of the configuration from sequence 1 to sequence 2 brings about a 6% decrease in predicted fatigue life. The reason for this decrease is analysed by plotting the reciprocal of the predicted crack propagation rate over crack length (dN/da, Fig. 9b), which is the number of cycles needed for growing the crack over a unit crack length.

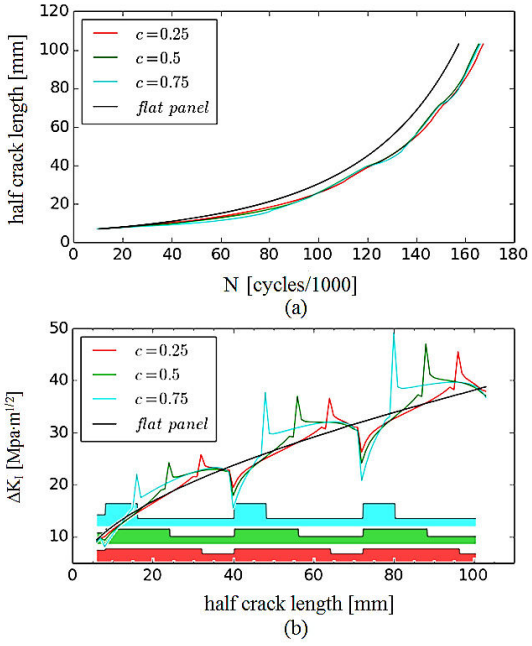

Fig. 8. (a) Predicted fatigue life of crenellated panels with different crenellation ratio in comparison with a flat panel with the same weight (b) the influence of crenellation ratio on the SIF profiles.

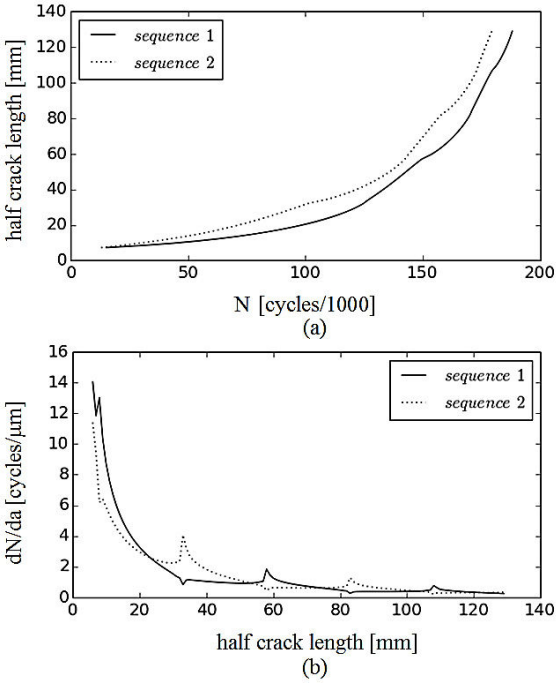

Fig. 9. (a) Comparison of predicted fatigue life between the crenellated panels with sequence 1 and sequence 2 configurations (b) number of cycles for crack growth over unit length at different half crack lengths.

As shown in Fig. 9b the dN/da value increases considerably when the crack length decreases below 40mm. Retardation occurs in this earlier period of crack growth is much more effective than retardation that occurs later. The acceleration due to thickness reduction in this region also causes more fatigue life loss. Thus the case with a crack firstly entering the thick region (sequence 1) will have a higher fatigue life gain. In order to achieve the highest fatigue life, there should be no thickness reduction region between the vulnerable sites for crack initiation like the root of stringers and the nearest pad-ups.

Table 2. Number of cycles needed to reach a given crack length for sequence 1 and sequence 2.

Half crack length [mm]	Cycles needed for sequence 1	Cycles needed for sequence 2
22	105198	77751
56	149467	142326
78	168308	155267
102	177904	171486
129	188814	179476

3.2.3 The influence of periodic length λ

The crenellation patterns with three different periodic lengths: 100 mm, 50 mm and 32 mm are investigated, which corresponds to 1, 2 and 3 times of complete repetitions of thick and thin regions within the 100 mm of crack growth (half length). All investigated patterns have the same crenellation ratio of 0.5 and the same configuration of 'sequence 1'. The fatigue lives predicted for the three crenellation patterns are compared in Fig. 10, which shows negligible influence of λ on the final fatigue lives.

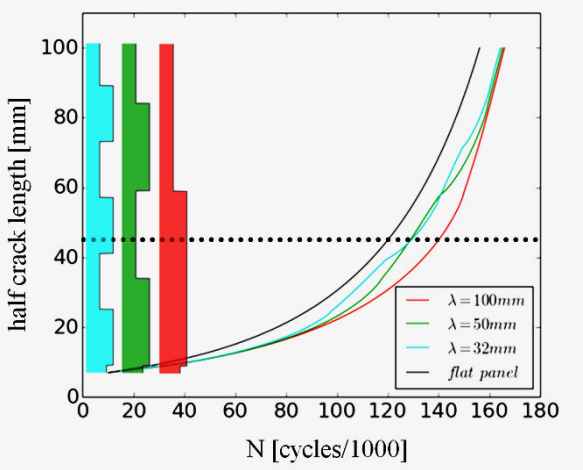

Fig. 10. Predicted fatigue life of crenellated panels with different periodic length.

However, when the half crack length is between 30 mm and 70 mm the crenellation pattern with λ = 100 mm has apparently longer fatigue life than the other two cases. This is due to the largest width of the pad-up in the case of λ = 100 mm, which gives an uninterrupted retardation in the first tens of millimetres of fatigue crack growth. The largest gain of fatigue life compared to the flat panel occurs at the half crack length of about 50 mm, where the crack tip is about to pass the retardation region in the pad-up.

4. Conclusions

In this work the geometric influence of crenellation patterns on the fatigue life of crenellated panel was analysed with the help of FE analyses. The three parameters: the crenellation ratio c, the periodic length λ and a position parameter were used to define the crenellation geometry. Their influence on the fatigue life was investigated separately and the conclusions are as follows:

1. If the thickness of the thin region is fixed, the fatigue life remains nearly constant with varying crenellation ratio in the range between 0.25 and 0.75.
2. An increased number of repetitions of thick and thin regions for a given length of fatigue crack growth does not change the fatigue life. However, when the periodic length is large enough to include the final crack tip inside the retardation region of the pad-up, significant fatigue life improvement can be achieved.
3. The pad-up at the small crack length has much more retardation effect than the same pad-up appearing at a larger crack length. As a result the initiation position of fatigue has considerable impact on the effectiveness of crenellations. It is recommended that if the possible crack initiation sites are known (e.g. the welding sites) the thickened regions of crenellations should be placed nearby.

Acknowledgements

The authors would like to thank Mr. Jürgen Knaack, Mr. Kay Erdman, Mr. Karl-Heinz Balzereit, Mr. Jie Liu and Mrs. Marianna Sticchi from the Department "Joining and Assessment" (WMF) of the Helmholtz Zentrum Geesthacht for their support in the experimental work and during the writing of the paper.

References

[1] M.-V. Uz, M. Koçak, F. Lemaitre, J.-C. Ehrström, S. Kempa, F. Bron, *Int. J. Fatigue*, **31** (2009).
[2] M.-V. Uz, *Improvement of Damage tolerance of Laser Beam Welded Aerospace Structures via Local Engineering,* Ph.D Thesis, Techischen Universität Hamburg-Harburg, 2010.
[3] S. E. Eren, M. Koçak, K. M. Nikbin, *International Conference on Advances in Welding Science and Technology for Construction, Energy and Transportation*, Istanbul, Turkey, 2010.
[4] R. Muzzolini, J.-C. Ehrstroem,, *The 15th Advanced Aerospace Materials & Processes Conference and Exposition AeroMat*, Seattle, USA, 2004.
[5] R. J. Bucci, *Aircraft Structrual Integrity Program Conference,* San Antonio, USA, 2006.
[6] J.-C. Ehrstroem, R. Muzzolini, S. Arsene, S. Van der Veen, *Proceedings of the 23rd Symposium of the International Committee on Aeronautical Fatigue*, Hamburg, Germany, 2005.
[7] S.M. Häusler, P.M. Baiy, S.M.O. Tavares, A. Brot, P. Horst, M.H. Aliabadi, P.M.S.T. de Castro, Y. Peleg-Wolfin, Structural Durability & Health Monitoring, **7** (2011) 3.
[8] M.-V. Uz, Y. J. Chen, *Proceedings of the 26th Symposium of the International Committee on Aeronautical Fatigue*, Montreal, Canada, 2011.
[9] L. Wang, W. T. Chow, H. Kawai, S. N. Atluri, *AIAA Journal,* **36** (1998) 3.
[10] U. G. Goranson, *In Proceeds of International Conference on Damage Tolerance of Aircraft Structures*, Delft, 2007.
[11] J. Lu, N. Kashaev, N. Huber, *Proceedings of the 29th Congress of the International Council of the Aeronautical Sciences,* Saint Petersburg, 2014
[12] S. Suresh, Fatigue of Materials, 2nd ed., Cambridge University Press, 2006
[13] ASTM *E647 Standard test method for measurement of fatigue crack growth rates.*
[14] R. Krueger, App. Mech. Rev., 57 (2004) 2.

Appendix

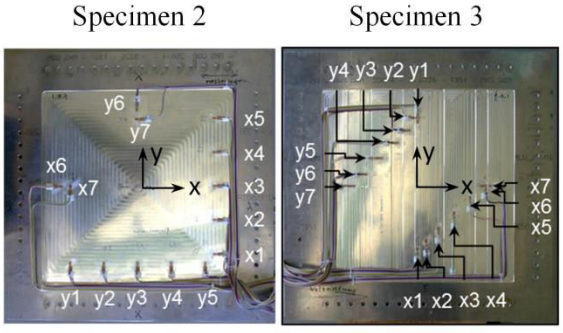

Fig. A1. Positions of strain gauges.

Table A1. Coordinates and orientation of strain gauges in specimen 2.

Strain gauges	Coordinates (x, y) [mm]	Orientation
x1	(160, -140)	a
x2	(160, -70)	a
x3	(160, 0)	a
x4	(160, 70)	a
x5	(160, 140)	a
x6	(-160, 0)	a
x7	(-140, 0)	b
y1	(-140, -160)	b
y2	(-70, -160)	b
y3	(0, -160)	b
y4	(70, -160)	b
y5	(140, 160)	b
y6	(0, 160)	b
y7	(0, 140)	a

Note: a - the strain gauge aligns with the major loading axes
b - the strain gauge aligns with the minor loading axes

Table A2. Coordinates and orientation of strain gauges in specimen 3.

Strain gauges	Coordinates (x, y) [mm]	Orientation
x1	(0, -133)	a
x2	(17, -116)	a
x3	(42, -91)	a
x4	(75, -58)	a
x5	(108, -25)	a
x6	(141, 0)	a
x7	(133, 0)	b
y1	(0, 133)	a
y2	(0, 141)	b
y3	(-17, 116)	b
y4	(-42, 91)	b
y5	(-75, 58)	b
y6	(-108, 25)	b
y7	(-133, 0)	b

Note: a - the strain gauge aligns with the major loading axes
b - the strain gauge aligns with the minor loading axes